MINISTRY OF AGRICULTURE, FISHERIES AND FOOD
DIRECTORATE OF FISHERIES RESEARCH

AQUATIC ENVIRONMENT PROTECTION: ANALYTICAL METHODS
NUMBER 9

An Automated NaI 'Well' Counting System for the Determination of Radiocaesium

D. J. Andrews and G. A. Sutton

LOWESTOFT

1993

The authors: D. J. Andrews MSRP and G. A. Sutton MSc MSRP are both Senior Scientific Officers.
At the time of writing both authors were based in Aquatic Environment Protection Division, Section 1 at Lowestoft. D. J. Andrews has since transferred to the Research Support Section, Electronics Group, also at Lowestoft.

Aquat. Environ. Prot.: Analyt. Meth., MAFF Direct. Fish. Res., Lowestoft, (9), 19 pp.

CONTENTS

Page

FOREWORD

1. Introduction 7

1.1 Sample preparation and geometry 7

1.2 Detector sensitivity and stability 7

1.3 Automatic sample changer 8

2. Materials and methods 8

2.1 Sample geometry 8

2.2 Choice of detector 8

2.3 Long-term spectral stability 10

2.4 Sample changer 11

2.4.1. Mechanical construction 12

2.4.2. Control panel, modes of operation and sample change sequence 13

2.5 Detector temperature controller 14

2.6 Shielding 15

3. Calibration 15

4. Results and discussion 16

4.1 Efficiency calibration 17

4.2 Minimum Detectable Activity (MDA) 17

4.3 Calculation of results of routine measurements 17

5. Conclusions 18

Acknowledgement 18

6. References 18

Appendix. . Example of Cs-134/137 results calculation 19

FOREWORD

As part of its responsibilities under various Acts of Parliament, MAFF Directorate of Fisheries Research has a duty to carry out a substantial programme of monitoring, surveillance and research in relation to the quality of the aquatic environment in and around the United Kingdom. In the course of that programme, a wide variety of methods of analysis are used for a wide variety of contaminants, both inorganic and organic, stable and radioactive. This series of publications describes the main methods used in the course of this work and parallels the existing Aquatic Environment Monitoring Report series, in which much of the resulting data is published. Regardless of whether the analytical procedure relates to a radionuclide or a non-radioactive contaminant, each report contains a step-by-step guide to analytical procedures and an explanation of the calculation of results.

P. W. Greig-Smith
Deputy Director
(Aquatic Environment Protection)
Ministry of Agriculture, Fisheries and Food
Directorate of Fisheries Research

1. INTRODUCTION

The determination of radiocaesium (Cs-134/137) in sea and fresh waters of the British Isles is part of the routine monitoring programme undertaken by the Ministry of Agriculture, Fisheries and Food (MAFF) at the Directorate of Fisheries Research (DFR), Lowestoft.

During the past five years the number of sea and freshwater samples collected by the DFR for radiocaesium analysis has increased significantly due to the extended monitoring programme following the Chernobyl accident. Counting times have increased because of the general reduction in levels of radioactivity following the introduction of a new effluent-treatment plant at British Nuclear Fuel's reprocessing plant at Sellafield. The large number of samples and the low levels of radioactivity have resulted in the requirement for an additional, highly sensitive, gamma counting system.

The existing 15 year-old system utilises a 12-position electro-pneumatic sample changer to place the sample within the 'well' of an inverted 127 mm by 127 mm Sodium Iodide (NaI) crystal detector assembly. Although this system has performed reasonably well it does have a number of shortcomings and is now requiring frequent maintenance. These shortcomings of the old system are associated with:

(a) *the detector* — high intrinsic background counts (mainly associated with K-40), relatively poor energy resolution of 12% at Cs-137 and sensitivity to small ambient temperature fluctuations causing spectral position changes; and

(b) *the sample changer* — poor repeatability of sample to detector positioning, problems with sample changer to detector alignment, some interference from adjacent samples, limited control options and inconvenience to use and maintain.

This paper describes the design and development of an improved automated gamma counting system suitable for the determination of low levels of radiocaesium activity in these samples.

Improvements in performance as compared with the existing DFR system were considered in the following areas:

- sample — preparation, geometry, and position with respect to the detector;
- detector — background, efficiency, energy resolution and stability; and
- sample changer — capacity, reliability, repeatable sample positioning and operational flexibility.

1.1 Sample preparation and geometry

The existing technique used to extract radiocaesium from water samples (Dutton, 1970; Baker, 1975) involves absorption of caesium on to silica-gel impregnated with ammonium molybdophosphate (ASG) contained in a 24 ml tubular plastic syringe sample container. Fifty-litre aliquots of filtered water are pumped through each ASG container. Careful appraisal of the various stages of this procedure, including sample geometry and homogeneity, failed to reveal areas where significant improvements could be made. Alternative ways of detecting caesium were investigated in the hope of being able to increase sensitivity; these were:

(a) a large volume of water was arranged to surround a 40%-relative efficient Germanium (Ge) detector to create a Marinelli beaker type of geometry; and

(b) a caesium sample in an ASG cartridge was positioned directly on a 30% efficient Ge detector cap.

In both cases, excessive counting times were necessary to obtain an acceptable precision of result as compared with the existing NaI 'well' detector system. Hence, it was decided to use a NaI(T1) 'well' detector for the new system, but to improve its performance as compared with the existing system in terms of background counts, efficiency, resolution etc. (see sub-section 2.2).

1.2 Detector sensitivity and stability

Samples containing low levels of radioactivity can be analysed successfully only if the signal due to the sample can be resolved from that of background radioactivity; an important requirement is that the operating temperature within the shield remains constant to maintain stable detector characteristics. The presence of natural radioactivity (e.g. K-40) has in this case been reduced by specifying very low background materials for the detector and using oxygen-free high-conductivity (OFHC) copper for the outer cladding.

The effect of cosmic and other high-energy gamma rays was reduced significantly by surrounding the detector assembly with a low background lead shield (127 mm thick) and filling the detector-access aperture with a cylindrical lead plug after each sample change.

Detector instability, due to fluctuations in the ambient operating temperature, was minimised by controlling the temperature of the detector housing using Peltier heat pump devices bonded to the detector assembly. A detector temperature of 19°C ± 0.2 °C was maintained over an ambient temperature range of 16°C to 31°C (sub-section 2.5).

1.3 Automatic sample changer

A detailed description of the new 20-position sample changer is given later (sub-section 2.4) but some of the salient features are:

(a) positive alignment of detector to sample changer mechanism, providing reproducible sample-to-detector geometry;

(b) pre-sensing of samples to enable empty positions to be ignored;

(c) use of a spring-loaded lead piston to shield the sample being counted and so reduce significantly the interference from adjacent samples, and also to ensure a good sample-to-detector geometry;

(d) sensitive over-current motor cut-out circuits to prevent damage from any physical obstruction; and

(e) a simple robust, well engineered design to provide a long, maintenance-free operation.

2. MATERIALS AND METHODS

Since the counting system is required to analyse many hundreds of sea and fresh water samples each year for radiocaesium, it is essential that the new system has:

- a high detection efficiency for radiocaesium;
- good energy resolution and high spectral stability;
- low intrinsic background; and
- a sample changer giving accurate repeatable and precise sample-to-detector positioning.

Particular attention was given to the features outlined above, and also to: sample volume, filtration technique, the caesium extraction process, the container type and its geometry, and the characteristics of the NaI 'well' detector.

2.1 Sample geometry

In trying to decide whether the existing sample container could be improved upon (i.e. ideally to extract more activity on to less ASG thereby enabling a smaller sample container to be used leading to a smaller detector 'well' and improved energy resolution and sensitivity) the sample preparation and radioactivity extraction techniques had to be studied in detail.

Sea and fresh water samples consist of up to fifty-litre aliquots of water. Each sample is filtered (using a 0.45 μm Millipore filter) and passed through a 24 ml tubular plastic syringe sample container containing a maximum of 10 g of ASG at a flow rate of 5 l h^{-1}. The caesium extraction efficiency is approximately 95% (Dutton, 1970) which is dependent on a maximum sample volume of 50 litres and a maximum flow rate through the ASG of 5 l h^{-1}. Mechanical difficulties arise when coping with sample volumes greater than 50 litres. The ASG containing the radioactive Cs-134/137 occupies about 16 ml of the 24 ml available in the sample container. The caesium activity is assumed to be distributed in such a way that the highest concentrations are to be found closest to the open end of the sample container, the concentrations reducing conically to a minimum at the closed end (Figure 1(a)). An homogenized caesium sample in half the volume (about 8 ml, Figure 1(b)) would present a more ideal source since, in addition to using the ASG more efficiently, it would create a much improved source-to-detector geometry. Various ways of homogenizing and compressing the ASG cartridge into a smaller volume were investigated but without success. The existing 24 ml tubular plastic syringe sample container and ASG geometry were therefore retained.

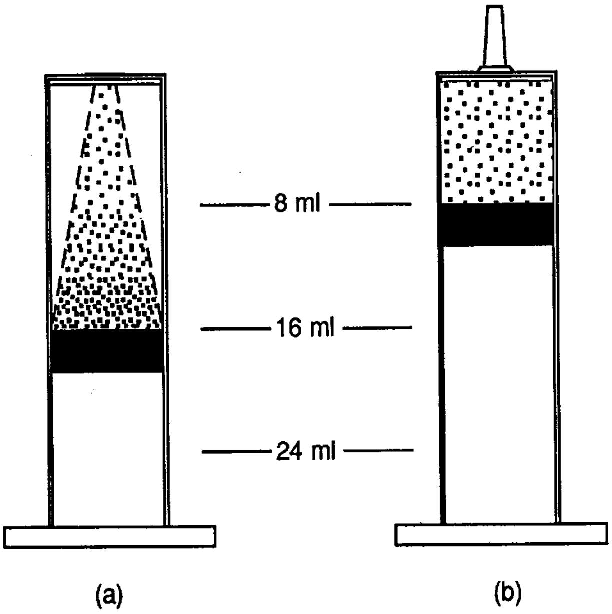

Figure 1. Sample tube geometry: (a) containing 16 ml of ASG, showing the estimated conical distribution of activity (dotted) with the nozzle removed from the top in readiness for entry into the detector 'well'; and (b) a more ideal sample geometry with 8 ml of ASG tightly packed with a uniform distribution of activity

2.2 Choice of detector

Many different configurations of NaI detectors are available commercially and the advantages and disadvantages of each were considered carefully before a final selection was made.

The performance of a NaI detector is a compromise between efficiency, shape, intrinsic background, and energy resolution. In general, the efficiency of a detector increases as the size of the crystal increases (to the point of total gamma absorption) but conversely, the intrinsic background increases and the energy resolution worsens.

Figure 2 shows efficiency curves for a range of thicknesses of NaI crystals. The photopeak energy of Cs-137 (0.662 MeV) is indicated by a dotted line. The efficiency for each crystal thickness can be determined from the abscissa. The 50 mm thickness has been identified as giving a good compromise between low intrinsic background, high efficiency, and economic cost.

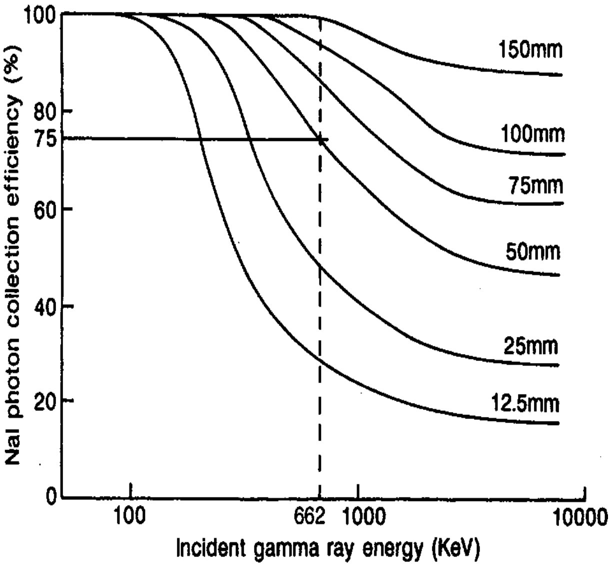

Figure 2. Collection efficiency for a range of NaI thickness. (From: Knoll, 1989)

Figure 3 shows the approximate relationship (at the Cs-137 photopeak energy) between NaI crystal thickness and photon collection efficiency; and between crystal thickness and active volume. The intrinsic background and cost of each crystal follow a similar increasing relationship to the active volume curve. Reduction of the background is particularly significant if very low levels of radioactivity are to be detected. It was concluded (from Figures 2 and 3) that the optimum NaI 'well' detector should have the following characteristics:

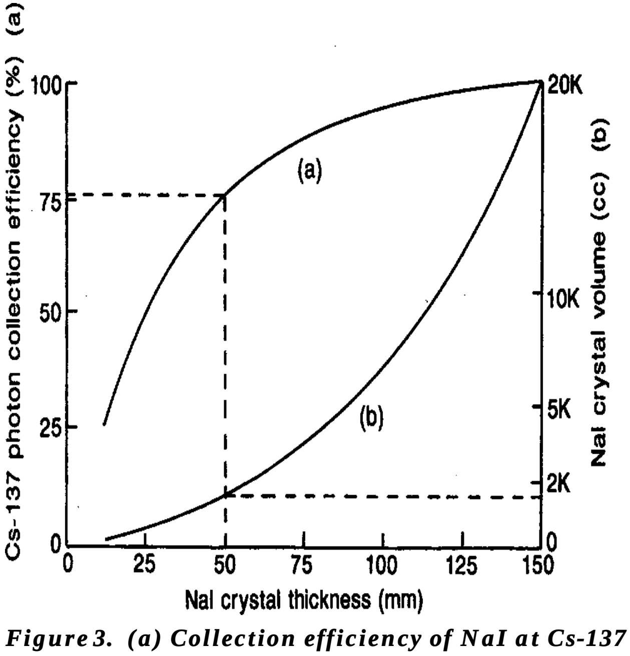

Figure 3. (a) Collection efficiency of NaI at Cs-137 line versus NaI crystal thickness; and (b) NaI volume versus NaI thickness

- crystal dimensions: 127 mm diameter by 127 mm; and
- 'well' dimensions; 25.4 mm diameter by 76 mm deep.

In addition, the crystal should be optically coupled via a quartz light pipe to a 75 mm EMI photomultiplier tube (PMT) with integral dynode chain and preamplifier, and the complete assembly clad in OFHC copper (see Figure 4). All other materials, other than the crystal, used for the construction were carefully selected to reduce the intrinsic background level of the assembly to a minimum.

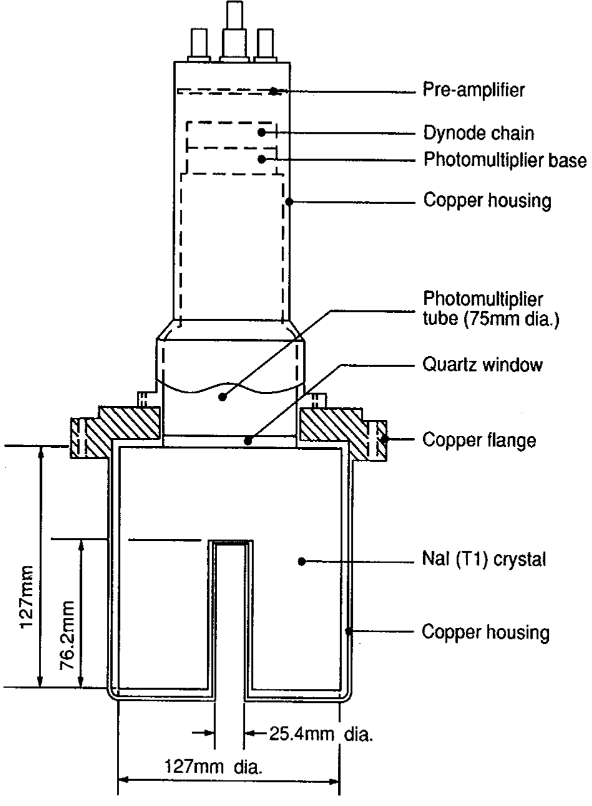

Figure 4. Detector assembly

For example, a 76 mm diameter photomultiplier tube was chosen instead of the 127 mm tube, the slightly lower photon-collection efficiency being easily compensated by the reduction in K-40 and other high-background components (Figure 5).

Additionally, before final construction of the counting system the manufacturer was requested to produce a crystal with 7% full width at half maximum (FWHM) resolution for Cs-137, in fact the detector received was specified as 8% for Cs-137. A comparison between the Cs-137 resolutions of the new and old detectors (Figure 5) shows that a resolution of 9% was achieved — 5(a), this was considered an acceptable improvement over the old detector FWHM figure of 12% — 5(b).

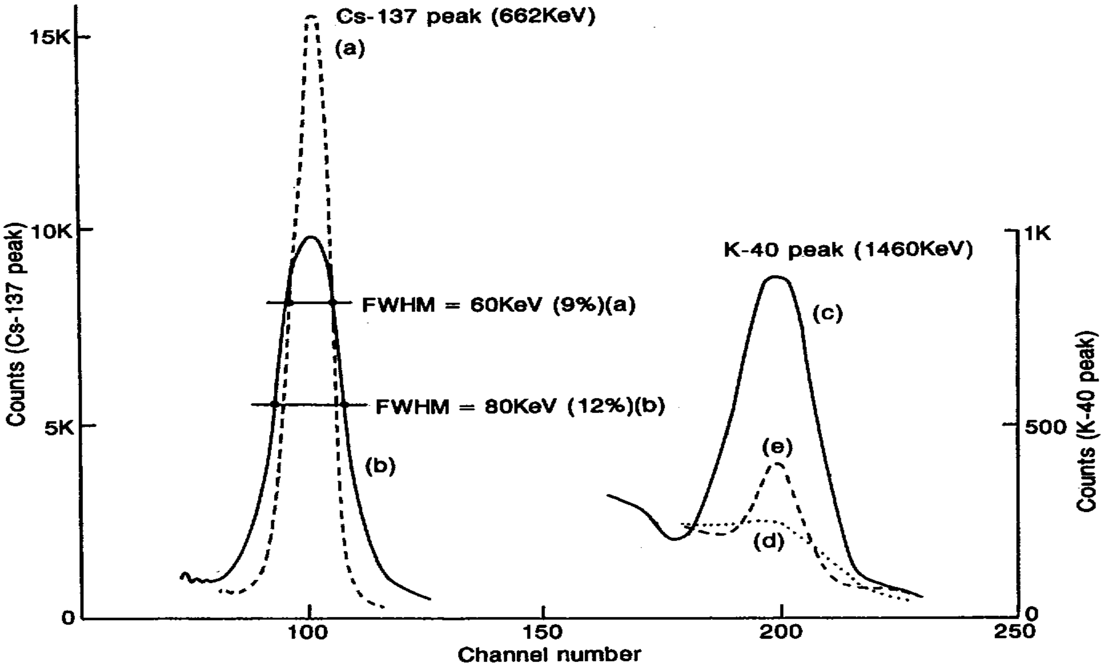

Figure 5. Comparison of detectors:
(a) new detector Cs-137 peak — 100 minute count *(using an identical source)*
(b) old detector Cs-137 peak — 100 minute count
(c) old detector K-40 peak — 100 minute count (blank tube)
(d) new detector K-40 peak — 1 000 minute count (empty tube)
(e) new detector K-40 peak — 100 minute count (blank tube)

2.3 Long-term spectral stability

Spectral stability is particularly important for the accurate determination of nuclides having multiple and interfering energy peaks, as any drift in the recorded location of an energy peak effectively worsens both resolution and accuracy and may invalidate the selected regions of interest and hence the calibration of the system. The overlapping peaks from Cs-134 (604 keV) and Cs-137 (662 keV) from a source of the two nuclides are shown in Figure 6. Accurate prediction of the shape of the two peaks and the calculation of the peak integrals (labelled A and C) and their respective background contributions (B and D), are totally dependent on the detector system's long-term, stable response to a known standard source. The contribution from Cs-134 at (A) is calculated from the Cs-134 peak integral at 795 keV (E) and associated background component (F).

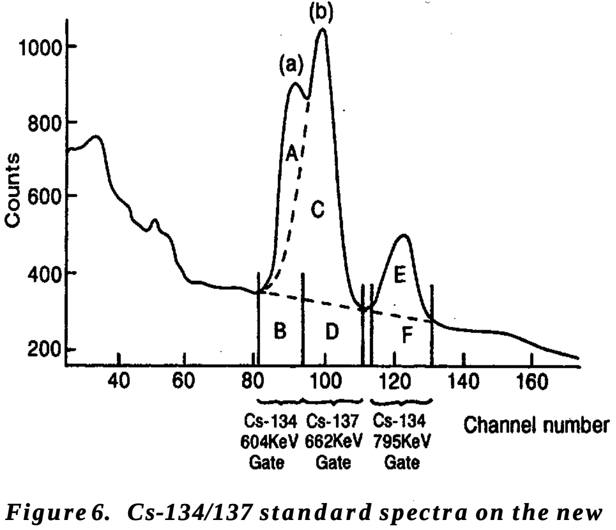

Figure 6. Cs-134/137 standard spectra on the new system

A NaI crystal and its associated PMT are highly temperature sensitive, even small temperature fluctuations cause voltage variations in the PMT output which translate to a shift in the gamma spectrum. The NaI crystal and PMT have positive and negative temperature coefficients respectively. As the PMT is the dominant element, the effect of a small positive temperature change will cause the spectrum to shift to the left (lower energy) and conversely, a decrease in temperature will shift the spectrum to the right (higher energy). The extent of this shift for the detector in question is approximately 7 keV per °C. The shift is significant for the range of temperatures experienced at the DFR Laboratory (daily fluctuations of about 4°C and seasonal fluctuations of 16°C to 26°C).

Spectral stability has been achieved by the novel design of a temperature stabiliser unit using Peltier cells (see sub-section 2.5). The unit maintains the detector assembly (NaI crystal and PMT) at a preset temperature of 19°C ± 0.2°C throughout an ambient temperature range of 16°C to 31°C. At this nominal temperature the crystal photon output efficiency is > 95% and also, since only 1°C below the mean ambient temperature, requires minimal regulatory effort from the Peltier stabiliser unit. The results of a three-day test of the prototype unit demonstrated that it was able to reduce a spectral shift of 7 keV per °C to less than 0.7 keV per °C. The greater stability achieved and the improvement in resolution (sub-section 2.2) enabled the regions of interest (ROI) or energy windows to be optimised to give a further reduction in background counts. Table 1 shows a comparison of the important parameters of the new and old systems.

2.4 Sample changer

The automatic sample changer unit is an electronically controlled mechanical device designed to hold twenty samples of nominal size 22 mm diameter by 80 mm length (equivalent to a 24 ml cylindrical plastic syringe). The samples are located in plated brass sample carriers on the periphery of a 460 mm diameter carousel. A linear-motion piston actuator pushes each sample up into the 'well' of the NaI detector under tension, and inserts a lead plug (50 mm diameter x 150 mm) into the shield aperture, this enables a constant source-to-detector geometry to be maintained and significantly reduces interference from adjacent samples. Hard wired CMOS (complemented metal oxide semi-conductor) logic is used for the control of the sample changer. A sample change is initiated via a 'trigger' input signal from the computer, during a sample change the output signal 'busy' is active. Figure 7 shows the complete system, Figure 8 shows a diagram of the main frame (the relative positions of the changer mechanism and shield can be seen).

Table 1. Comparison of new and old 'well' systems

Parameter	Units	Old system	New system
1. MCA settings	Channels	256	256
	KeV/Ch	9.0	6.5
2. Standards	Cs-137 Gross	1 560 cpm	1 523 cpm
	Net	1 481 cpm	1 498 cpm
		(Channel 87-112)	(Channel 89-109)
3. Backgrounds	30 KeV-1.66 MeV	789 cpm	252 cpm
	Cs-137 window	79 cpm	25 cpm
	K-40 window	98 cpm	7.4 cpm
4. Resolution	Cs-137 FWHM	(12%) 80 KeV	(9%) 60 KeV
	Co-60(1)	2.6:1	4.0:1
5. Adjacent sample interference (2)		0.008%	0.006%
6. Figure of merit(3)	Cs-137 standard	18.7	60.0
	Sample no.6824	0.28	2.7
7. Shielding	Lead(4)	100 mm	130mm
~~8. Crystal size~~		~~127 x 127 mm~~	~~127 x 127 mm~~

(1) *Peak to trough ratio*
(2) *Interference from adjacent sample positions*
(3) *Calculated using signal to background ratios*
(4) *Mean thickness of lead around detector*

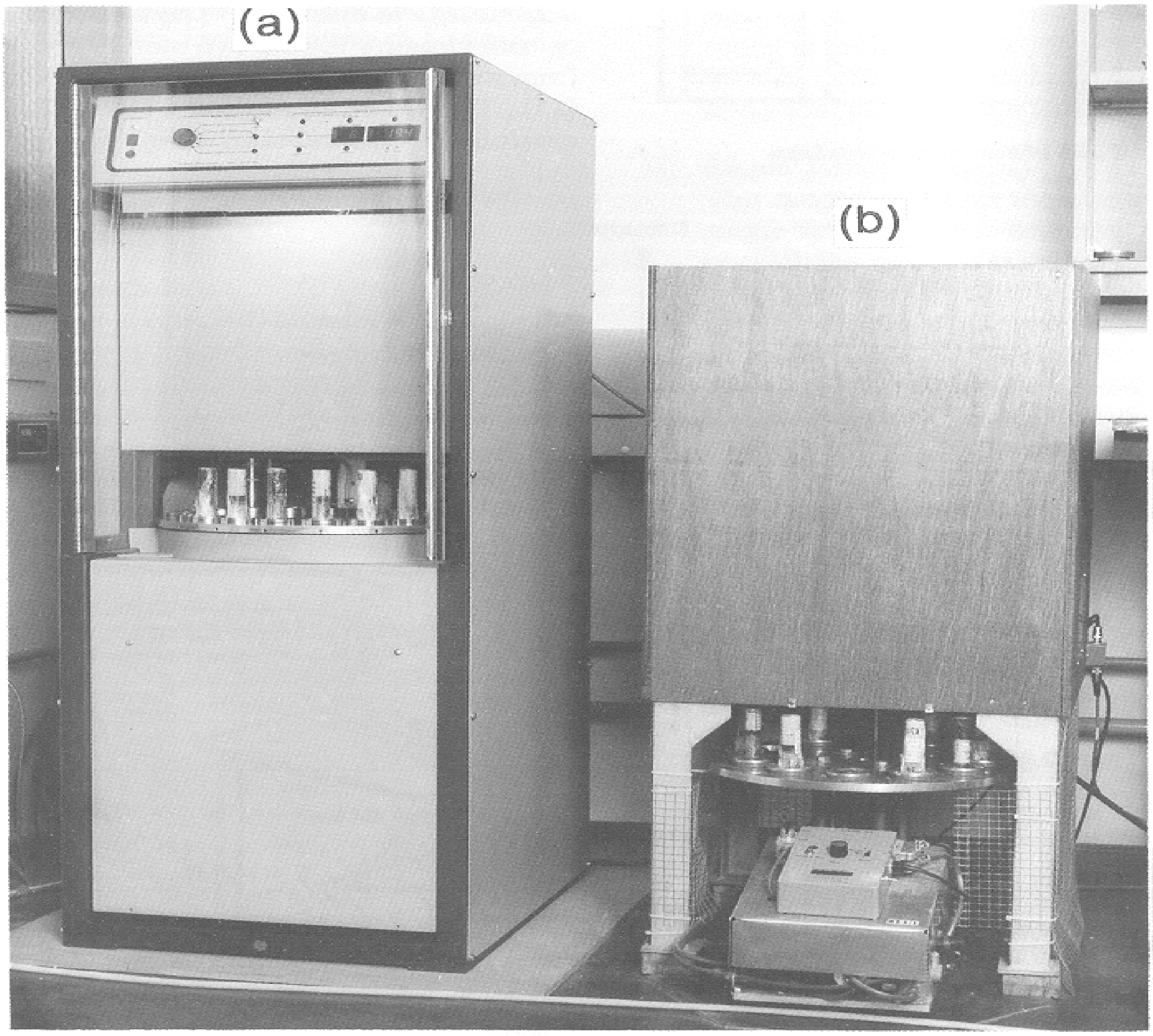

Figure 7. Overall view showing: (a) the new NaI 'well' counting system; and (b) the old NaI 'well' counting system

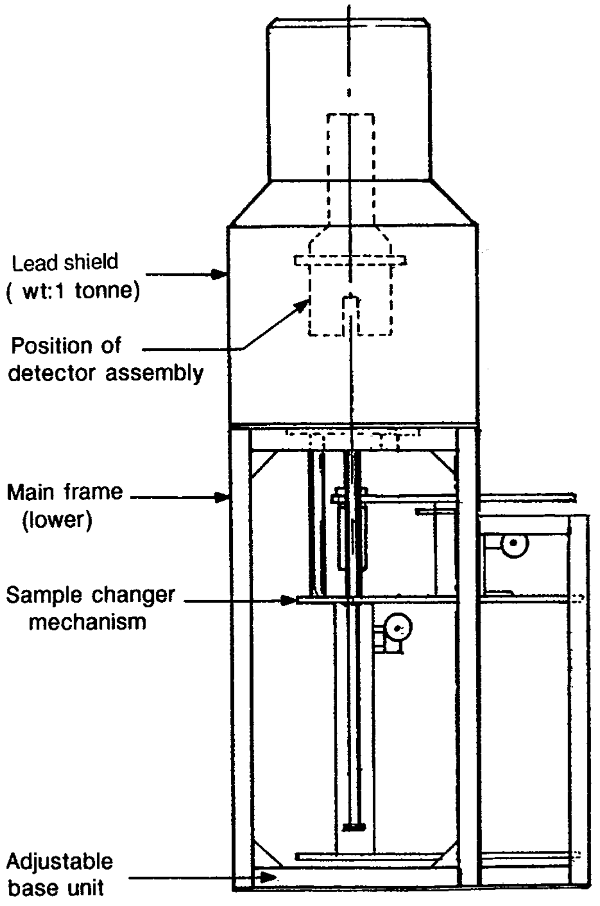

Figure 8. Side view of the system

2.4.1 Mechanical construction

The sample changer unit is self-contained and can be withdrawn from the main enclosure for access and maintenance. It is mounted on an adjustable base plate and raised by means of an adjusting screw to enable positive location with the shield and detector assemblies.

Figure 9 shows a sketch of the complete mechanism which comprises a twenty-position carousel (1) and bearing assembly (2), mounted on the main frame consisting of top, centre and base plates (3, 4 and 5) which are connected by support pillars (6). The carousel is rotated by a 12 VDC drive unit (7), its position being controlled by an opto-sensor (8). Twenty samples (9) and sample carriers (10) are located in holes on the periphery of the carousel, sample presence is sensed by another opto-sensor (11). A linear shaft, piston-drive assembly (12 and 13) mounted between the base and centre plates uses a spring-loaded lead piston (14) to lift a sample and sample-carrier about 300 mm into the detector/ shield assembly. The electrical power and control circuitry for the two motors is supplied from a controller unit situated on the base plate (15). The power unit for the Peltier temperature controller is also mounted on the base plate (16).

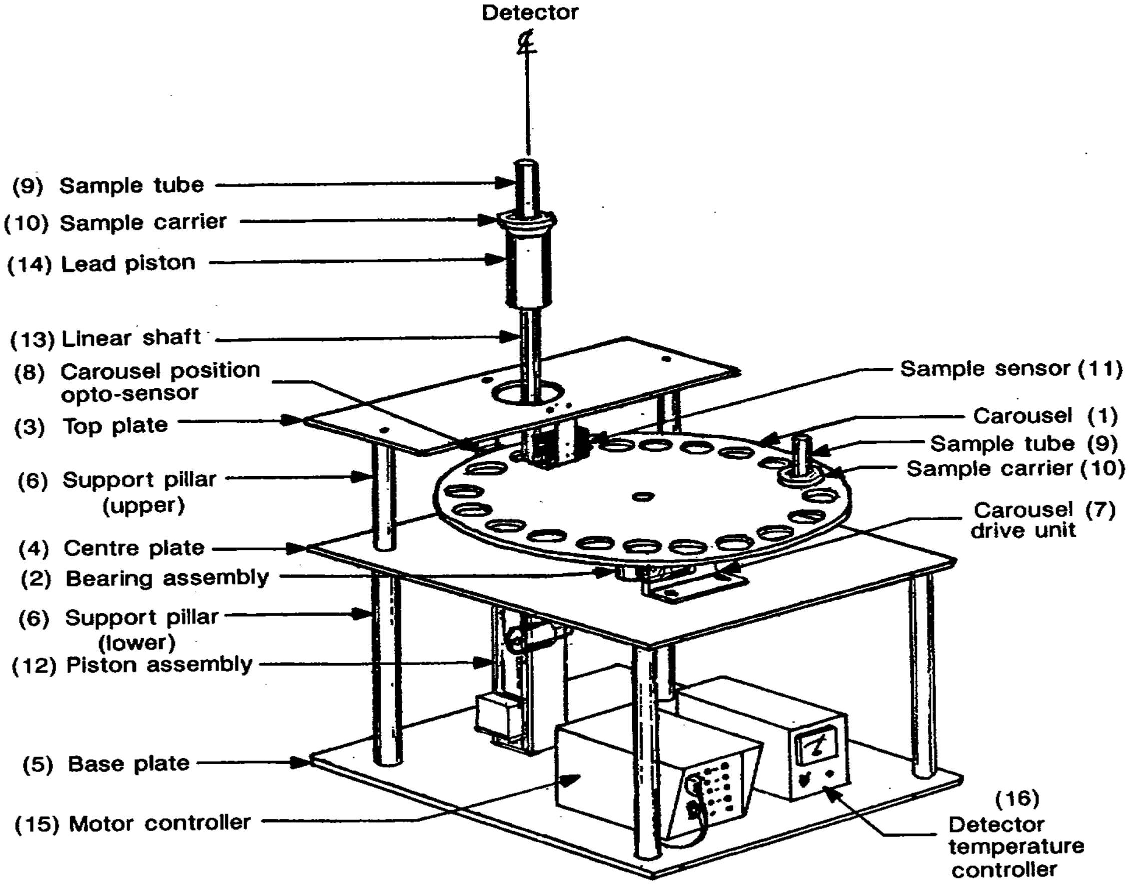

Figure 9. The sample changer mechanism

2.4.2 *Control panel, modes of operation, and sample change sequence*

The sample changer system electronics is divided into two principle areas: the sample changer logic circuitry and motor controller, and the detector temperature controller. The sample changer control unit (which contains the logic control circuitry), the sample number display and logic power supply boards, and the operator's control panel, are located in the upper part of the system enclosure. (The operation of the temperature controller is explained in detail in sub-section 2.5.)

The operator's control panel (Figure 10) is divided into three distinct sections: mains, mode select, and status. The mains section includes an on/off switch, mains fuse and indicator light. The mode section employs a rotary switch to select one of five possible modes of operation, a push-button to initiate rotation of the sample carousel and a two-position toggle switch to select between single or repeat counting of a sample. The status section comprises the sample number display (and a reset button), and the detector temperature display with an indication of heating or cooling status. Other indicators are: sample out, in or in-transit, carousel indexing, temperature controller operating, and sample indexing cycle complete.

The mode select switch is a 5-position rotary switch with the following facilities:

(a) Autocycle (Repeat)
When autocycle is selected the sample beneath the detector aperture is automatically raised into the detector well by the piston assembly. The sample remains in this position until the sample changer receives a trigger pulse (Figure 11) which causes the mechanism to lower the sample from the detector to the carousel, index to the next sample and raise this one into the detector 'well'. The sequence will continue indefinitely whilst trigger pulses are received. During a sample change cycle the output signal 'busy' is active.

(b) Autocycle (Single)
This mode is similar to Autocycle (Repeat) except that the sequence is terminated after one full rotation of the carousel (i.e. sample number 20 has been counted and removed from the detector), the cycle 'complete light' is then illuminated.

(c) Manual Index (Single)
The mode for manually loading samples onto the carousel. When selected, a sample within the detector is automatically lowered to the carousel. The carousel may then be indexed one position at a time, by a momentary operation of the 'manual' push button switch. The sample number display can be reset to 1 in this mode only.

(d) Manual Index (Continuous)
This is similar to the Manual Index (Single) mode except that the carousel rotates continuously until another mode is selected.

(e) Auto Test
This mode is used for testing the operation of the sample changer mechanism. When selected, the sample carrier beneath the detector aperture is raised to the detector 'well'. Sample change cycles are then generated automatically approximately every four minutes until another mode is selected.

(f) Single Sample (Repeat)
This mode is used for the repetitive counting of a single sample. When selected, the sample beneath the detector is raised into the detector 'well'. On receipt of a 'trigger' pulse (count period completed) the sample remains in position since the 'busy' signal simulates a sample change cycle by being active for approximately the same length of time as a normal sample change. A new count period is then initiated.

A brief description of the automatic mode sequence is as follows (Figure 11): the 'trigger' signal initiates the piston motor to lower a sample, microswitch S6 opens

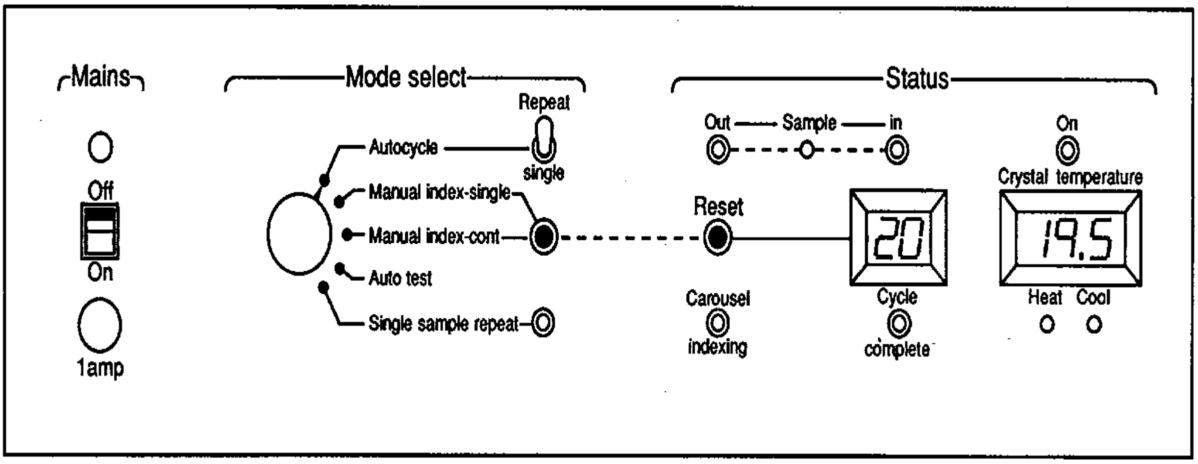

Figure 10. The control panel layout

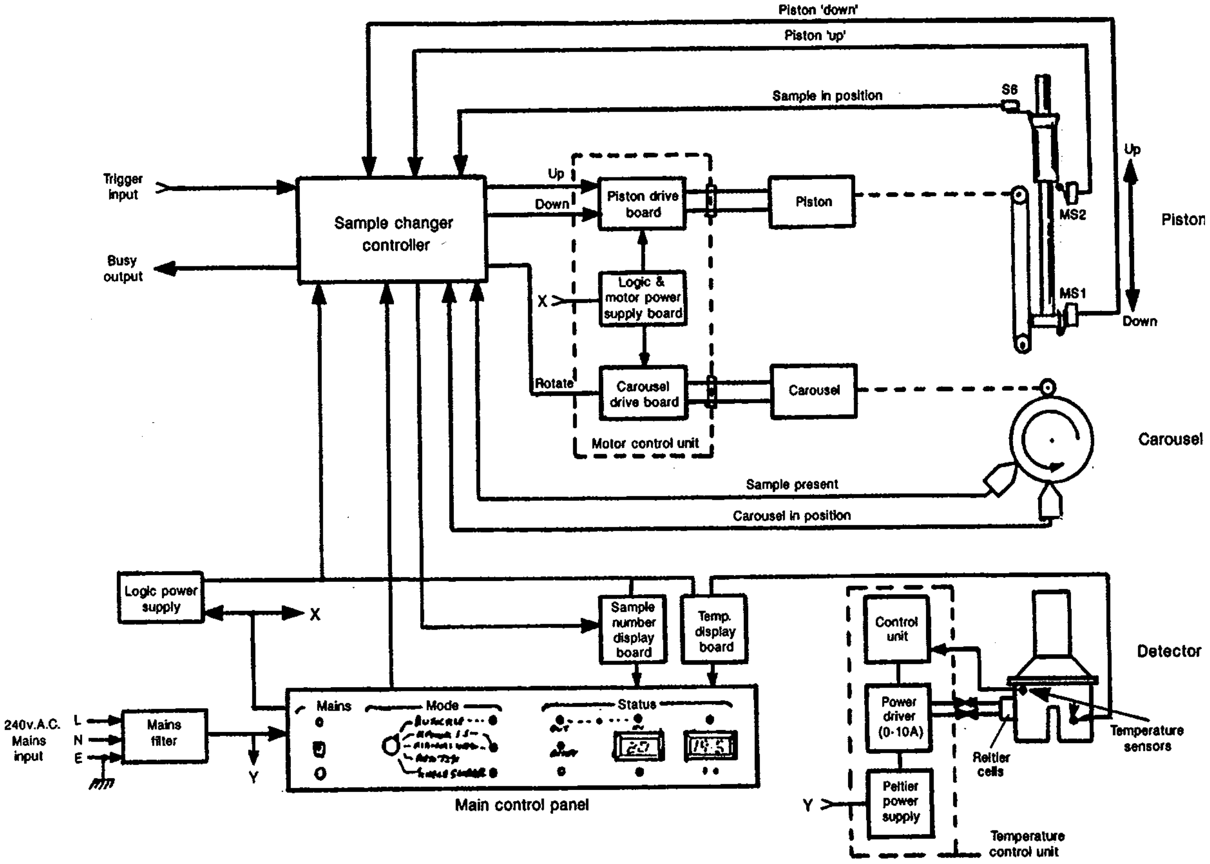

Figure 11. Control system block diagram

activating the 'busy' signal, and MS2 operates. When the piston is fully lowered MS1 operates and the carousel-rotate motor starts. The carousel rotates until the next sample is sensed by an opto-device, it stops when the position opto-device is activated. The piston motor operates and raises a new sample into the detector. Microswitch S6 operates de-activating the 'busy' signal, and subsequently MS2 operates to switch off the piston motor. The sample number indicator increments by 1 for each sample loaded into the detector.

2.5 Detector temperature controller

The detector temperature controller comprises three Peltier heat pump cells bonded thermally to the copper housing of the detector. Peltier devices heat or cool depending on the direction of current flow. The cells are energised by a 0 to 10 ampere low-voltage current source, and controlled by a platinum-film temperature sensor (also bonded to the detector housing). A schematic diagram of the control system is shown at Figure 12(a). Temperature control is achieved by regulating the current flow to the device to be either: in the forward direction, in the reverse direction, or absent. The current flow status is indicated by two light emitting diodes (LEDs) on the front panel.

The temperature of the detector is indicated using the circuit shown in Figure 12(b). A separate platinum

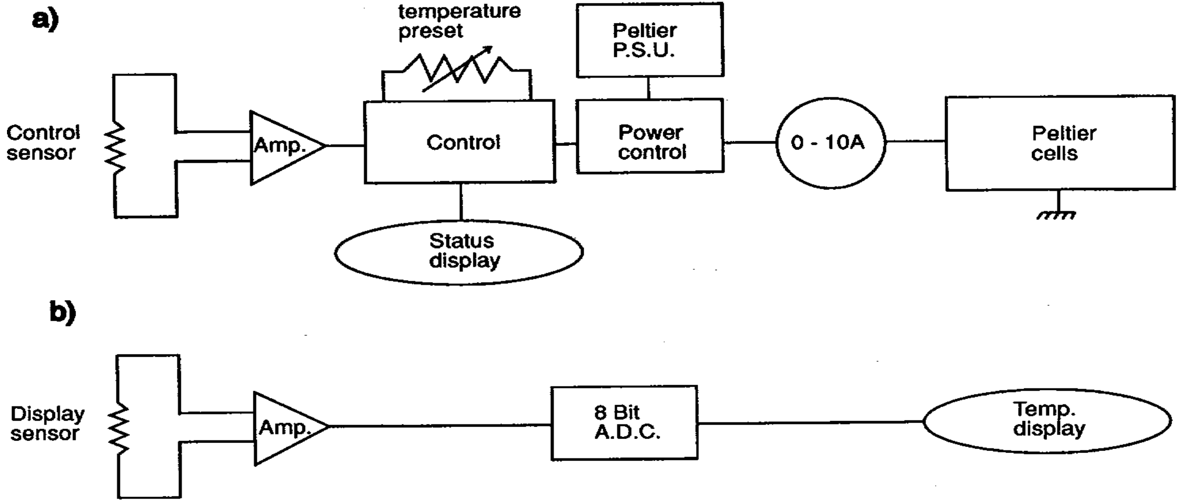

Figure 12. (a) Temperature control system block diagram
(b) Temperature display system block diagram

temperature sensor is bonded to the detector housing and coupled via a bridge amplifier and an eight-bit analogue to digital converter (ADC) to a digital display on the front control panel.

2.6 Shielding

The NaI detector is shielded using a low background, cylindrical lead cave comprising twenty-seven 25 mm thick-stepped lead rings having a lower diameter of 457 mm and an upper diameter of 305 mm (Figure 13). The base thickness of the cave is 152 mm, and the lower wall, upper wall, and top wall thicknesses are 125 mm, 100 mm, and 100 mm respectively. The total weight of the lead shielding is approximately 1 000 kg.

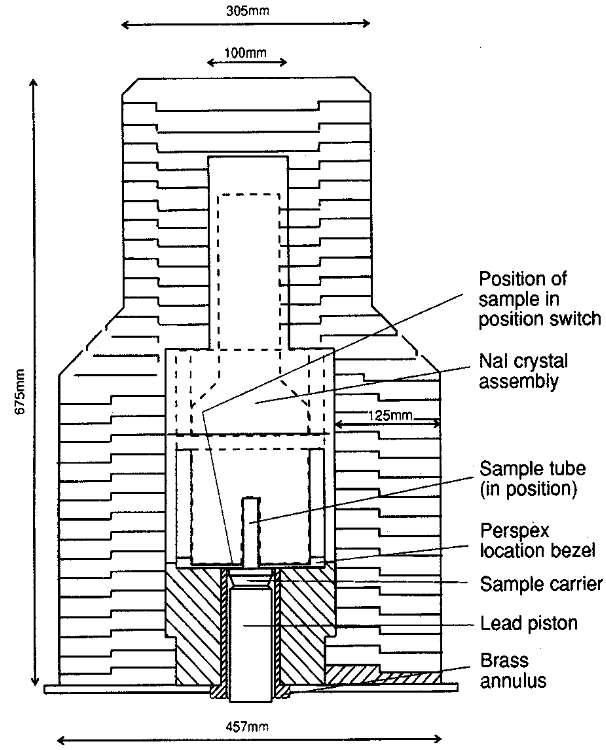

Figure 13. The new 'well' cylindrical lead shield

3. CALIBRATION

The calibration of a spectrometric system comprises two clearly defined areas:

- determination of the energy *versus* channel number relationship; and
- determination of the energy *versus* efficiency relationship.

A meaningful calibration can be achieved only if the calibration samples closely simulate the normal environmental samples. Hence, careful preparation of the calibration samples is essential and identical materials and containers must be used throughout.

The relationship between nuclide gamma energy and channel number was achieved by using three radioactive sources containing Co-60, Cs-134/137, and K-40. The ADC, amplifier settings and high voltage settings, were adjusted so that the Cs-137 energy (0.662 MeV) and the Co-60 energy (1.332 MeV) peaks occurred at channel numbers 100 and 200 respectively for convenience, and also so that zero energy coincided with channel number zero. An energy range of 33.3 keV (channel number 5) to 1.70 MeV (channel number 256) was achieved (i.e. a linear response of 6.66 keV channel^{-1}) (Figure 14). The calibration optimised the number of

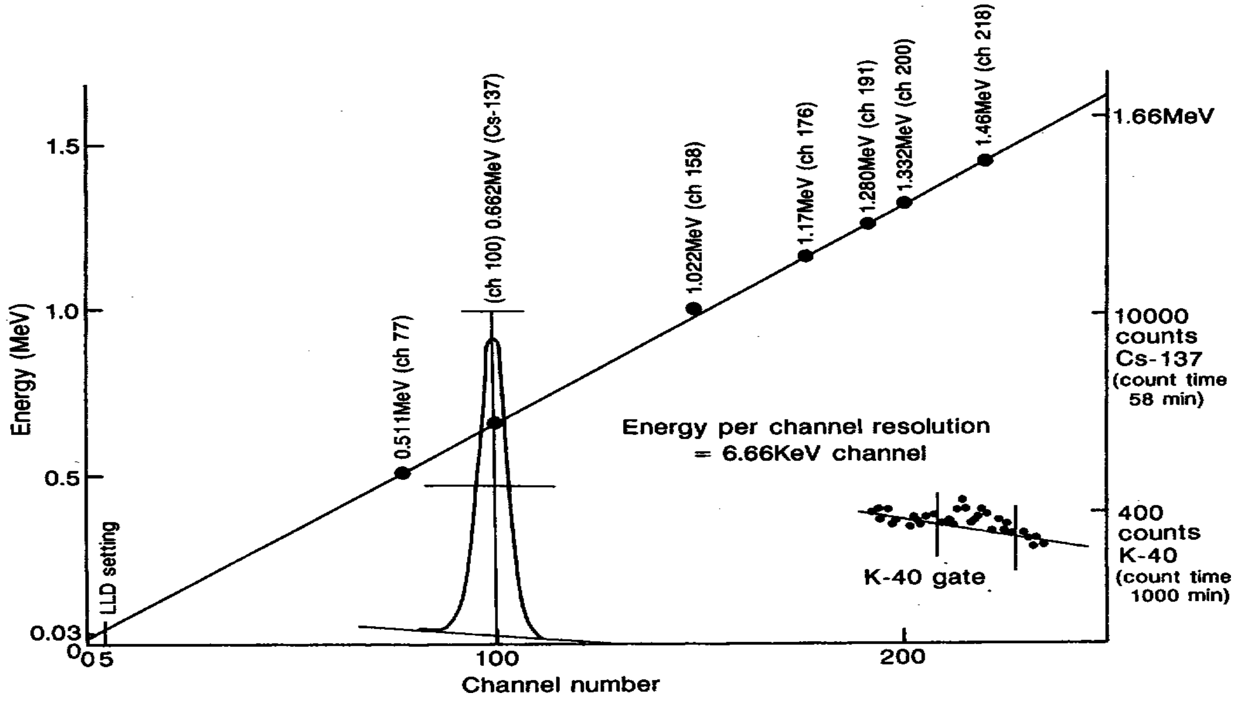

Figure 14. Calibration graph of energy versus channel for the new system

channels so as to describe adequately the two caesium peaks and also provide sufficient high energy channels to accommodate the K-40 peak at 1.46 MeV (channel 218).
The relationship between energy and efficiency was obtained using the following procedure:

(i) Ten sample containers, each containing 5 g of ASG reagent, were dried thoroughly over a period of 24 hours.

(ii) A 'Blank' sample was prepared by adding distilled water to one of the above sample containers until the ASG reagent was thoroughly dampened. The amount of water added (about 3 ml) was determined by weighing the sample container before and after addition.

(iii) Standard radioactive solutions (specific activity about 0.5 Bq ml^{-1}) were prepared containing Cs-137, Cs-134, and Cs-137 plus Cs-134. Aliquots of these solutions were added to the remaining sample containers to produce three of each radioactive solution. The geometry of these nine 'standard' sample containers were consistent with 'normal' samples as the same preparation procedure had been followed.

(iv) All ten cartridges were carefully labelled and dated.

Initially, each sample was counted for one hour to check for any inconsistencies in the preparation process. From the counting data a mean and a 1-sigma standard deviation was calculated. Those falling outside the 1-sigma limit are normally discarded, however for this calibration all fell within the limits. The sample which approximated most closely to the mean was chosen to be used for the final calibration.

4. RESULTS AND DISCUSSION

The caesium calibration standards prepared in Section 3 above were used to obtain three gamma spectra (Figures 15, 16 and 17). A linear response of 6.66 KeV channel^{-1} was obtained for the system (Figure 14). A comparison of background count rates (using an empty sample container) between the old and the new NaI 'well' counting systems (Table 1) shows clearly the dramatic reduction in background achieved by the new system. These reductions are evident across the entire energy spectrum and particularly noticeable in the K-40 gate (Figure 5(c), (d) and (e)). The data in Table 1 using an empty sample container may be compared with a similar set of results (Table 2) obtained using the 'Blank' sample prepared in Section 3 above. This shows a significant improvement; for example, the Cs-137 background is reduced from 71 cpm for the old system to 25.5 cpm for the new system.

The results from the standards prepared in Section 3

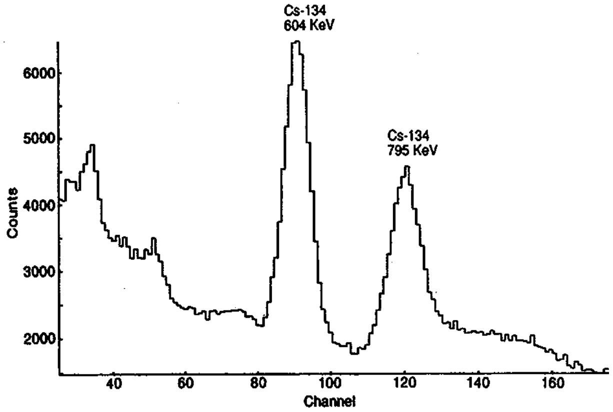

Figure 15. The response of the new system to Cs-134 standard

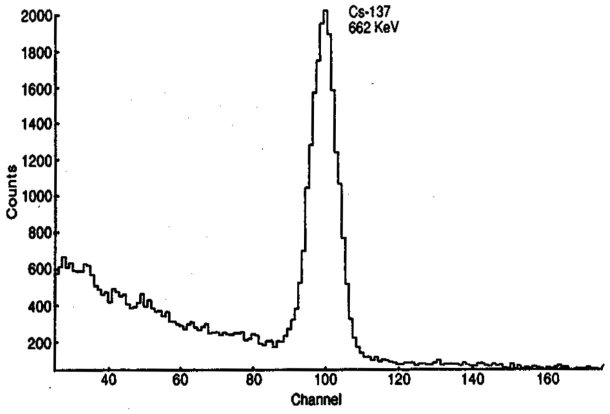

Figure 16. The response of the new system to Cs-137 standard

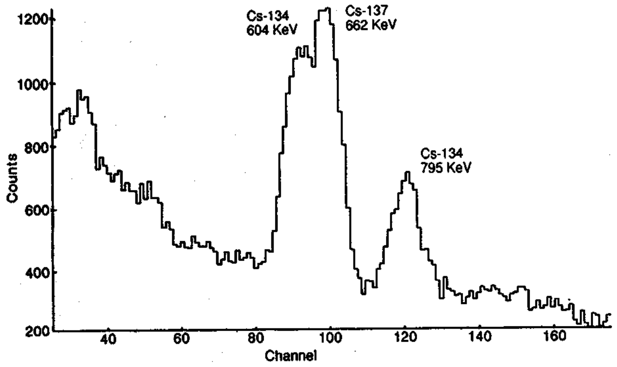

Figure 17. The response of the new system to Cs-134+137 standard

Table 2. Caesium background data for new and old NaI 'well' systems using a 'Blank' sample tube

	Cs-137(1)	Cs-134/ 137(2)	Cs-134	Units
New system	25.5	29.8	11.4	cpm
Old system	71.0	100.4		46.2 cpm
ROI width (3)	87-112	85-114	115-130	channel number
Peak energy	662	604 and 662	795	keV

(1) Region of interest used for Cs-137 when Cs-134 peak at 795keV has not been detected

(2) Region of interest used for Cs-137 when Cs-134 peak has been detected at 795 keV and Cs-134 component needs to be subtracted from the Cs-134/137 unresolved integral (see Figure 6)

(3) Width of region of interest (or window) used to calculate peak integrals on the new system

were used to calculate the counting efficiency for Cs-137 and Cs-134, and also to determine the minimum detectable activity (MDA) of the system.

4.1 Efficiency calibration

The detector efficiency of a counting system $E_{(E)}$ is given by the equation:

$$E_{(E)} = \frac{n_{(E)}}{R_{(E)}} \qquad (1)$$

where $n_{(E)}$ is the count rate (number of counts in the peak channels divided by the counting time), and $R_{(E)}$ is the rate at which photons of energy *(E)* are emitted from the source. (It should be noted that this efficiency relates only to a specific source/detector geometry and radionuclide).

Nationally traceable standards of Cs-137 and Cs-134 were purchased from Amersham International plc. The standards were quantitatively diluted and presented to the counting system in the usual sample geometry and counted until sufficient counts had been accumulated to ensure an error of < 1%. The efficiency was calculated for each sample and the result that approximated most closely to the mean result was selected for use in the activity calculations. The mean system efficiencies were determined as: Cs-137 = 36.6% and Cs-134 = 11.4%.

It is important to note that however thoroughly the samples are mixed, some heterogeneity is always evident. Hence, the individual sample efficiency closest to the mean is considered to have the greatest homogeneity and thus the one most suitable for a quantitative efficiency determination

4.2 Minimum Detectable Activity (MDA)

The MDA of a counting system is defined as the amount of activity that must be present such that there is a finite probability < P_1 of declaring that there is **no** activity when in fact there **is**, and also that there is a probability < P_2 of declaring that there **is** activity present when in fact there is **not**. If P_1 is set equal to P_2, then:

$$\text{MDA} = \text{F x } 2k \text{ x } \sqrt{2\text{B}} \qquad (2)$$

where *B* is the total background count within the particular caesium peak;

k the required error probability factor (obtained from tables of one-tailed distribution data), and

F the factor to convert counts to activity (involves duration of count, decay, decay scheme factor, efficiency, etc.).

Typical values for k are shown in Table 3.

Table 3. Table of k-factors for typical error probabilities

Probability of making an error (P)	k-factor
≤ 0.05	1.645
≤ 0.01	2.326
≤ 0.005	2.576

If P is selected as P ≤ 0.05 then k = 1.645 which when substituted in equation (2) yields:

$$\text{MDA} = \text{F x } 4.66 \text{ x } \sqrt{\text{B}} \qquad (3)$$

The mean background count-rate for Cs-137, based on a 400 minute count, is 26.08 cpm (i.e. B = 26.08 x 400, and the count time = 400 x 60 seconds). Substituting in equation (3), (excluding factor F) gives an MDA of 0.0198 cps. Finally, if the efficiency factor F which for the new system is 1/0.366, is substituted in equation (3), then the MDA = 54mBq (total activity of sample).

If a similar substitution is made for the old ‘well’ system (where B = 70.37 x 400, and the count time is 400 x 60 seconds) then the MDA (excluding factor F) = 0.0326 cps. Including the old system factor F produces an MDA of 88 mBq (total activity of sample).

Since each water sample is usually 50 litres, the MDA values may be considered to be 1.08 mBq l^{-1} and 1.76 mBq l^{-1} for the new and old ‘well’ counting systems respectively.

4.3 Calculation of results of routine measurements

The results are calculated using the raw spectral data from the Cs-134/137 region of interest (see Table 2) and efficiency and background as in sub-section 4.1 above. The calculation also includes correction factors for ASG batch recovery, abundance, decay, and sample volume. Each batch of samples counted also includes a standard and two background tubes to provide a system efficiency check and a running mean background respectively. The basic formula for calculating the results in mBq l^{-1} is:

where *cpm* = sample counts per minute minus background counts per minute.

The analysis system produces results in mBq l^{-1} and are either given as Cs-137 (only) or Cs-137 and Cs-134. When a Cs-137 (only) result is produced it means that Cs-134 has not been detected and the narrower region of interest can be used (see Table 2) for the Cs-137. When a Cs-134 and a Cs-137 result is produced it means that

Cs-134 at 795 KeV has been detected and a proportional number of counts have to be subtracted from the Cs-134/137 unresolved peak integral to obtain the Cs-137 result (see Figure 6 and Table 2).

All results are scrutinised by an analyst, all those results falling below the systems MDA of 1.08 mBq l^{-1} (or any other pre-determined level) are discarded.

An example of a typical results calculation for a nominal 50 litre seawater sample is given in the Appendix.

5. CONCLUSIONS

The initial aims of designing and constructing a new caesium NaI 'well' counter with an improved performance have been achieved. Significant reductions to its intrinsic background were achieved using a Peltier temperature-controller to maintain the NaI detector and PMT assembly at a constant temperature.

Also, the carousel capacity has been increased by 70% and a re-designed controller and actuator mechanism incorporated. This has enabled better use to be made of 24-hour and weekend counting periods, as well as far greater flexibility of control (individual regimes for samples, background and standards, repeat counts, special test and loading modes, etc.).

The most significant enhancement is the 63% increase in sensitivity (i.e. the capability of the system to detect lower levels of activity for the same counting time). Since about 40% of our environmental samples are now very near the MDA value of the old system (i.e. 1.76 mBq l^{-1} for a 400 minute counting time), the MDA of the new system (1.08 mBq l^{-1} for a 400 minute counting time) has enabled an improved assessment to be made of the sample activity of this increasing number of low-level samples.

Finally, the new NaI 'well' counting system in its modern housing has proved to be a most reliable, versatile and sensitive counting system and has justified fully the time and effort spent on its design and implementation. It is proposed to use the experience to refurbish the old 'well' system which will include not only the novel features of the new system, but also a microprocessor controller to enable even greater, and remote control of the entire counting process.

Acknowledgement

The authors would like to acknowledge the time and thought given by Bicron Corporation, via Nuclear Data Inc. (UK), for the manufacture of a suitable detector assembly.

6. REFERENCES

DUTTON, J. W. R., 1970. The determination of radiocaesium in sea and fresh water. Tech. Rep. Fish. Radiobiol. Lab., MAFF Direct. Fish. Res., Lowestoft (FRL), (***6***): 9 pp.

BAKER, C. W., 1975. The determination of radio-caesium in sea and fresh water. Tech. Rep. Fish. Radiobiol. Lab., MAFF Direct. Fish. Res., Lowestoft (FRL), (***16***): 8 pp.

KNOLL, G. F., 1989. Radiation Detection and Measurement. John Wiley and Sons, New York, 754 pp.

APPENDIX. Example of Cs-134/137 results calculation

Count time = 48 000 seconds

Cs-134 integral (channel 115-130) = 9460 = 11.83 cpm
Cs-137 integral (channel 85-114) = 27842 = 34.80 cpm
Cs-137 (only) integral (channel 87-112) = 24555 = 30.69 cpm

Background counts Cs-134 = 11.81 cpm
(running mean) Cs-137 = 30.13 cpm
Cs-137 (only) = 26.09 cpm

NET integral count Cs-134 = 0.015 cpm
rates Cs-137 = 4.673 cpm
Cs-137 (only) = 4.604 cpm

Cs-134 in Cs-137 1.5866 x 0.015 = 0.024 cpm
correction factor (K)
Subtract from Cs-137 4.6725 - 0.0238 = 4.649 cpm

Correcting for ASG batch recovery (r), efficiency (Eff) and abundance (y) gives:

	cpm		r		cpm x r	Eff/y	cpm x r/Eff x y
Cs-134	0.015	x	1.022	=	0.153	0.120	0.128
Cs-137	4.649	x	1.022	=	4.751	0.365	13.023
Cs-137	4.673	x	1.022	=	4.775	0.362	13.198

Decay correction

$e^{0.693}$ x Decay time (days)/half life

$e^{0.693}$ x 201.66/11012 = 1.204 (Cs-137)

$e^{0.693}$ x 201.66/751.9 = 1.013 (Cs-134)

Therefore: Cs-134 = 1.204 x 0.128 = 0.154 cpm
Cs-137 = 1.013 x 13.023 = 13.192 cpm
Cs-137 (only) = 1.012 x 12.198 = 13.370 cpm

Converting to mBq l^{-1} (1 000/60 x Vol) where volume = 50.3 l.

Giving final results of:

Cs-134 = 0.154 x 0.331 = 0.05 mBq l^{-1}
Cs-137 = 13.192 x 0.331 = 4.37 mBq l^{-1}
Cs-137 (only) = 13.370 x 0.331 = 4.43 mBq l^{-1}

(K) *= ratio of abundance of Cs-134 795 KeV peak to 604 KeV peak*

RECENT AQUATIC ENVIRONMENT PROTECTION: ANALYTICAL METHODS

No. 1 Analytical procedures for the determination of neptunium radionuclides in marine waters, sediments and biota.

No. 2 Methods of analysis of hydrocarbons in marine and other samples.

No. 3 Methods of analysis for trace metals in marine and other samples.

No. 4 The determination of total tin and organotin compounds in environmental samples.

No. 5 Analytical procedures for the determination of strontium radionuclides in environmental materials.

No. 6 Methods of analysis for chlorinated hydrocarbons in marine and other samples.

No. 7 The determination of alpha-emitting nuclides of plutonium, americium and curium in environmental materials: Part 1. Sea water.

No. 8 The determination of technetium-99 in environmental materials.